

Nanoelectromechanical torsion switch of low operation voltage for nonvolatile memory application

Wenfeng Xiang^{1,2} and Chengkuo Lee^{1,a)}

¹Department of electrical and computer engineering, National University of Singapore, 4 Eng. Drive 3, Singapore 117576

²Department of Mathematics and Physics, China University of Petroleum, Beijing 102249, People's Republic of China

(Received 30 November 2009; accepted 16 April 2010; published online 13 May 2010)

Nanoelectromechanical torsion switches are fabricated by using focused ion beam milling on silicon-on-insulator substrate. The device layer thickness of the substrate is 220 nm. A 9 μm long and 1.5 μm wide suspended silicon cantilever is mechanically connected to peripheral silicon device layer via a silicon torsion spring with the length of 2.4 μm and width of 530 nm. After hydrofluoric-acid vapor releasing, the silicon cantilever shows downward deflection. The pull-in voltage is about 5.5 V and the ratio of current measured at the ON/OFF states is over 1000. Moreover, the simulated data of pull-in voltage of torsion switch is in agreement with the experimental result, which will contribute to design of an optimal nanoelectromechanical torsion switch with a driven voltage as low as 1.2 V. According to the preliminary results, this torsion switch with low driven voltage has a great potential for high density non-volatile memory application.

© 2010 American Institute of Physics. [doi:10.1063/1.3428781]

The pursuit of manufacturing ever miniaturized complementary metal-oxide-semiconductor (CMOS) microelectronics has been progressively increasing and offering continuous improvement in circuit performance during the past three decades. However, many challenges were encountered as CMOS technology is scaled into the fundamental limits, for example, power dissipation, gate oxide leakage, and short channel effects.^{1,2} To introduce the materials and device structures such as high-K oxide and one-dimensional structures based on nanotube, nanowire, and nanoribbon into the Si platform is a promising solution to realize nanoelectronics as the next-generation microelectronics. Recently several nanoelectromechanical system (NEMS) switches have been explored intensively for nonvolatile and random access memory applications in terms of advantages such as high operating speed and low driving voltage.³⁻⁷ Carbon nanotube (CNT) based NEMS switches show excellent switching characteristics. Jang *et al.*⁸ reported the vertical three-terminal CNT-based switches operated at pull-in voltage of 22–25 V. When the distance between gate and drain of CNT-based switch was decreased to 30 nm, the pull-in voltage reduced to 4.5 V distinctly.⁹ Kaul *et al.*⁶ reported the switching time of 2.8 ns which was measured in the two-terminal CNT-based devices. However, it is a challenge to precisely control the number and specific location of CNTs in large areas by the conventional CMOS process technology.

By using standard CMOS process technology, Jang *et al.* reported TiN-based NEMS cantilever switches with the dimension of $200 \times 300 \times 30\text{nm}^3$ in width, length, and thickness and the gap between electrodes of 15 nm.⁵ The pull-in voltage is slightly higher than 10 V. Nevertheless, it is difficult to reduce pull-in voltage for this normal cantilever switch when device dimension is down to nanometer scale. The pull-in voltage of the TiN-based NEMS switches re-

ported in Ref. 5 is not obviously improved when the cantilever length (CL) is increased from 300 to 500 nm. To have a NEMS switch which is actuated by the state-of-the-art CMOS integrated circuits (IC), we reported a NEMS switch with torsion spring driven at a low voltage.

Figure 1(a) shows the NEMS torsion switch fabricated

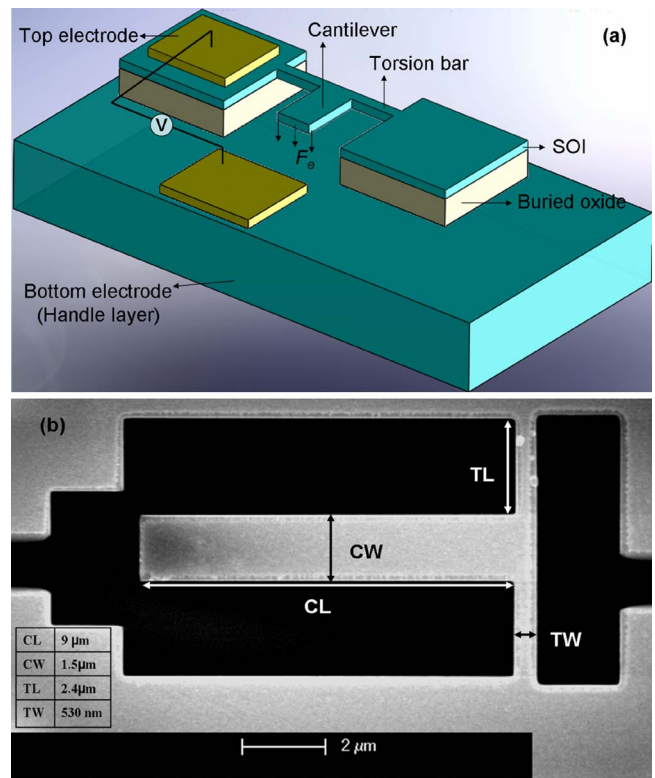


FIG. 1. (Color online) (a) A schematic illustration of the NEMS torsion switch device. (b) SEM photo of a NEMS torsion switch after HF vapor releasing. The CL, CW, TL, and TW of device are 9 μm , 1.5 μm , 2.4 μm , and 530 nm, respectively.

^{a)}Author to whom correspondence should be addressed. Electronic mail: elelc@nus.edu.sg.

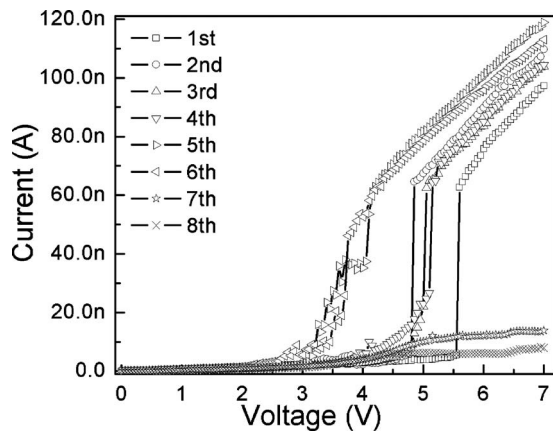


FIG. 2. I - V characteristic of the device shown in Fig. 1(b) in multiple operations.

on a silicon-on-insulator (SOI) wafer with a thin device layer of 220 nm and 2 μm buried oxide layer. The device layer and handle layer of SOI wafer are heavily doped in n-type to achieve low resistivity (~ 0.01 – $0.02 \Omega \text{ cm}$). After contact area opening of handle layer of SOI wafer, the Cr (10 nm)/Au (100 nm) layers were deposited as the top electrode on the device layer and the bottom electrode on the handle layer of SOI wafer. The NEMS torsion switch comprising a suspended silicon cantilever supported by a torsion spring is etched from the device layer by using the FEI Nova 600 focused ion beam (FIB) system with a low 30 pA ionic current to assure a high resolution and a good reproducibility. After FIB milling, the NEMS torsion switch is released using hydrofluoric-acid (HF) vapor etching technique to avoid the cantilever stiction. Figure 1(b) shows a scanning electron microscopy (SEM) photo of the NEMS torsion switch after HF vapor releasing while the CL and cantilever width (CW), and torsion spring length (TL) and width (TW) of torsion switch are 9 μm and 1.5 μm and 2.4 μm and 530 nm, respectively. It shows that the cantilever of torsion switch is downward deflected after HF vapor releasing step. Such result enabled a gap between the cantilever end and the bottom electrode.

When a voltage is applied on the cantilever and bottom electrode of NEMS torsion switch, an electrostatic field will be formed. If the field is strong enough, the electrostatic force (F_e) will push the cantilever down to bottom electrode by twisting the torsion spring. The switching of ON/OFF states of switch is mainly determined by force balance between F_e and mechanical restoring force of torsion spring (F_s). The “ON state” is defined as the state of that the free end of cantilever is pulled down to contact the bottom electrode when the F_e overcomes the F_s . The cantilever will switch back to the initial state (OFF state) after the driving voltage is removed.

The I - V curves of the device under multiple operations in air ambient are shown in Fig. 2. In the first-cycle measurement, it is observed that the current increases sharply at about 5.5 V and linear I - V curve is obtained at the voltage above 5.5 V, in which it indicated there is an Ohmic contact. The OFF-state current is found to be very low ($\sim 0.1 \text{ pA}$ level). Thus we concluded that the ON/OFF current ratio is exceeding 1000. The pull-in voltage decreased slightly, while the I - V characteristics are degraded distinctly after the fourth-cycle measurement, which is resulted from charging

effect possibly. Regarding the dynamic behavior of torsion switch, F_e is balanced by F_s before the cantilever bending angle reach the pull-in angle. When the cantilever bending angle reaches the pull-in angle, the current sharply increases because the cantilever touched the bottom electrode immediately.¹⁰ In our NEMS switch, the cantilever and bottom electrode are silicon. After HF vapor releasing, there is residual native oxide on surface of the cantilever and bottom electrode. During the electrical measurement, holes/electrons will be charged into the surfaces and an additional electrostatic force is formed. The cantilever does not return to the initial state after the applied voltage is removed. It means that the gap distance between the free end of cantilever and bottom electrode decreased. From the seventh-cycle measurement, the I - V curves changed and no obvious current jump occurred. The change in conductive behavior of I - V curves is needed to be investigated deeply. One of the possible reasons is that the active area of charge distribution on the cantilever surface increased. Owing to the decrease in the gap distance between the free end of cantilever and bottom electrode by the charging effect, the area of charge distribution is larger than that of the previous-cycle measurement when the voltage is applied. Therefore, the charge density of unit area on the cantilever surface decreases and the strength of electrostatic field in the gap reduces, which is resulted in the decreased current. In Jang’s report, the TiN-based NEMS switch was repeatedly operated over 300 times and the pull-in voltage is stabilized at 13 V with the variation within 1 V.⁵ In order to improve the switching characteristic of proposed torsion switch, we may deploy TiN or silicide to replace the silicon as the cantilever materials in future study.

As shown in Fig. 1(b), there is downward deflection of the cantilever end. The atom force microscopy (AFM) measurement shows the distance between the free end of cantilever and the bottom electrode of torsion switch after HF releasing is only about 80–100 nm. Therefore, the torsion spring is twisted in the initial state with rotated angle of ~ 0.206 – 0.208 rad after HF vapor releasing. The mechanical torque of torsion switch with the same dimension of prepared device was simulated using ABAQUS finite element modeling. Figure 3(a) shows the mechanical torque of ideal torsion switch without pretwisted torsion spring as the function of the rotated angle. Nonlinear relationship is observed for the variation in mechanical torque regarding the rotated angle. As shown in Fig. 3(a), the mechanical torque of torsion switch can be calculated using the equation as follows:

$$M(\theta) = 7.5376 \times 10^{-11} \theta + 1.9486 \times 10^{-11} \theta^2, \quad (1)$$

where θ is the cantilever bending angle between the NEMS cantilever plate and handle layer plate. Figure 3(b) shows the electrostatic torque under different applied voltage as well as the mechanical torque for the prepared NEMS torsion switch. MAXWELL is used to simulate the electrostatic torque of NEMS switch. When a 5.5 V voltage is applied on the NEMS switch, the rotated angle of the cantilever shown in Fig. 3(b) exhibits two physical solutions. However, no solution is given when the applied voltage is higher than 6.5 V. It can be concluded that the simulated pull-in voltage is about $\sim 6 \text{ V}$. The simulated pull-in voltage is slightly larger than the experiment result, which is possibly resulted from estimation error of the pretwisted angle in the initial state of NEMS switch.

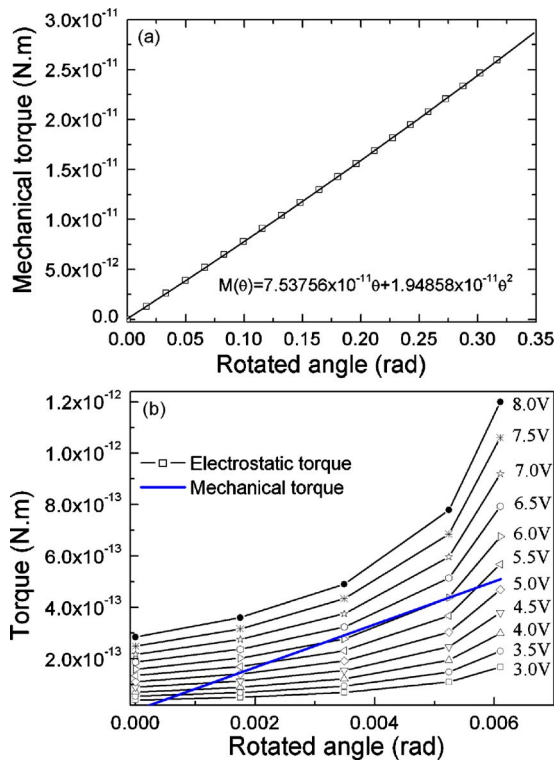


FIG. 3. (Color online) (a) The simulated mechanical torque-rotated angle for the NEMS torsion switch. In the initial state, the torsion bar has not been pretwisted. (b) The mechanical torque and the electrostatic torque applied on the fabricated NEMS torsion switch. In the initial state, the torsion bar is assumed to be pretwisted for 0.207 rad.

Compared to conventional cantilever switches, one of the advantages of NEMS torsion switch is that the dimension of cantilever and torsion spring can be separately controlled and optimized so as to achieve small pull-in voltage. In other words, the electrostatic force can be increased by using large cantilever plate, while the mechanical torque of torsion spring can be reduced simultaneously by having nanoscale torsion spring. Owing to the thick buried oxide layer in SOI wafer, the problem of cantilever deflection during the HF vapor releasing is difficult to control. It is observed that device geometry has an important influence on the cantilever deflection during HF releasing of device. Moreover, the simulation model helps us to optimize the device structure to get a NEMS switch with low-driven voltage. For example, a torsion switch fabricated by SOI wafer with dimension like CL of 2 μm , CW of 1.5 μm , TL of 1.5 μm , TW of 200 nm, the gap of 50 nm, and the thickness of torsion spring of 70 nm. If we assumed that the torsion switch has not been pretwisted, the simulated pull-in voltage shown in Fig. 4 is about 1.2–1.3 V. It can be seen that narrower gap between two electrodes and softer torsion spring are the keys for enabling lower operation voltage compared to the fabricated device shown in Fig. 1(b). Therefore the NEMS torsion switch with an optimal structure is able to decrease the pull-in voltage to satisfy the requirement of nonvolatile memory devices.

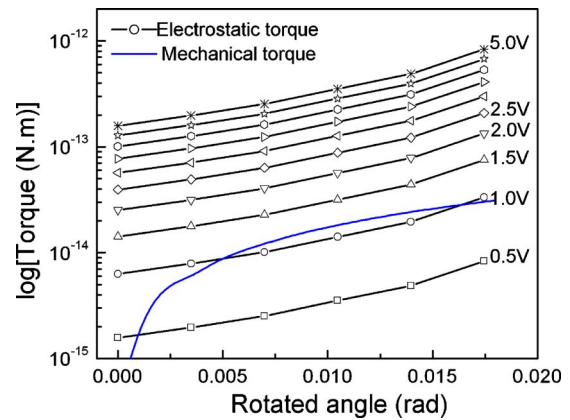


FIG. 4. (Color online) The mechanical torque and the electrostatic torque applied on a model of NEMS torsion switch. In this NEMS switch model, TL is 1.5 μm , TW is 200 nm, CL is 2 μm , and CW is 1.5 μm , the thickness of torsion spring is 70 nm and the distance between the free end of cantilever and bottom electrode is 50 nm.

In summary, a NEMS torsion switch has been prototyped by using FIB milling. In the initial state of just-prepared NEMS torsion switch, the cantilever of device is downward deflected and the gap distance between cantilever end and the bottom electrode is about 80–100 nm measured by AFM. The pull-in voltage is about 5.5 V and the ratio of current measured at ON/OFF states is over 1000. In addition, the simulated pull-in voltage of torsion switch is in agreement with the experiment result. By optimizing the device structure, the proposed NEMS torsion switch can be expected as one of the promising candidates for nonvolatile memory applications of next-generation IC.

This work has been support by the National University of Singapore under Grant No. R-263-000-475-112. The authors thank Professor Fu-Li Hsiao, Dr. Bin Yang, and Dr. Yu Du for useful discussions.

- ¹V. V. Zhirnov, P. K. Cavin, J. A. Hutchby, and G. I. Bourianoff, *Proc. IEEE* **91**, 1934 (2003).
- ²D. J. Frank, R. H. Dennard, E. Nowak, P. M. Solomon, Y. Taur, and H. P. Wong, *Proc. IEEE* **89**, 259 (2001).
- ³T. Rueckes, K. Kim, E. Joselevich, G. Y. Tseng, C. L. Cheung, and C. Lieber, *Science* **289**, 94 (2000).
- ⁴J. E. Jang, S. N. Cha, Y. J. Choi, D. J. Kang, T. P. Butler, D. G. Hasko, J. E. Jung, J. M. Kim, and G. A. J. Amaratunga, *Nat. Nanotechnol.* **3**, 26 (2008).
- ⁵W. W. Jang, J.-B. Yoon, M.-S. Kim, J.-M. Lee, S.-M. Kim, E.-J. Yoon, K. H. Cho, S.-Y. Lee, I.-H. Choi, D.-W. Kim, and D. Park, *Solid-State Electron.* **52**, 1578 (2008).
- ⁶A. B. Kaul, E. W. Wong, L. Epp, and B. D. Hunt, *Nano Lett.* **6**, 942 (2006).
- ⁷K.-T. Lam, C. Lee, and G. Liang, *Appl. Phys. Lett.* **95**, 143107 (2009).
- ⁸J. E. Jang, S. N. Cha, Y. Choi, G. A. J. Amaratunga, D. J. Kang, D. G. Hasko, J. E. Jung, and J. M. Kim, *Appl. Phys. Lett.* **87**, 163114 (2005).
- ⁹J. E. Jang, S. N. Cha, Y. Choi, T. P. Butler, D. J. Jang, D. G. Hasko, J. E. Jung, Y. W. Jin, J. M. Kim, and G. A. J. Amaratunga, *Appl. Phys. Lett.* **93**, 113105 (2008).
- ¹⁰O. Degani, E. Socher, A. Lipson, T. Leitner, D. J. Setter, S. Kaldor, and Y. Nemirovsky, *J. Microelectromech. Syst.* **7**, 373 (1998).